

https://doi.org/10.1070/QEL17278

Limiting spectral and angular characteristics of multilayer relief–phase diffraction microstructures

G.I. Greisukh, E.G. Ezhov, A.I. Antonov, V.A. Danilov, B.A. Usievich

Abstract. **Methods for estimating the parameters of relief–phase diffraction microstructures (local and integral *Q*-factors) are extended to the case of multilayer double-relief sawtooth microstructures, which makes it possible to select the best combinations of optical materials for multilayer microstructures at a very low computational burden. An approach to the study of multilayer microstructures is proposed, based on the combined use of *Q*-factors and the method of rigorous analysis of coupled waves, which allows one to estimate the limiting spectral and angular characteristics of multilayer microstructures of various types.**

Keywords: *diffractive optical element, multilayer relief–phase diffraction microstructure, diffraction efficiency, scalar and rigorous diffraction theory.*

1. Introduction

Diffractive optical elements (DOEs), due to their unique aberration properties, are of considerable interest for imaging optical systems designed to work with polychromatic radiation. Indeed, a single DOE with a small optical power coupled into the refractive lens objective, makes it possible to achieve a high degree of chromatism correction necessary to obtain a high-quality colour image, even for a limited set of optical materials from which refractive surfaces can be made by precision stamping [1–5]. However, the dependence of diffraction efficiency (DE) on the wavelength and the angle of incidence of the light at the DOE, as well as the technological difficulties that accompany the suppression of this dependence, are still a serious obstacle to a wide practical use of DOEs in such systems. Here, of course, we primarily mean the lenses of photo and video cameras of mobile devices and security cameras for mass production, the lenses of which are replicated today by precision stamping. Therefore, a competitive technology for applying a sawtooth relief–phase microstructure with suppressed spectral and angular energy dependences onto a spherical or aspherical refracting surface would undoubtedly open the way to the widespread introduction of refractive-diffraction optics in the mass production of high-quality photo and video cameras.

Known effective solutions for weakening the dependence of DE of a sawtooth relief–phase microstructure on the wavelength and the angle of incidence of the light on an element suggest a transition from single-layer sawtooth microstructures to structures containing several layers and reliefs [6–14], as shown in Figs 1 and 2.

G.I. Greisukh, E.G. Ezhov, A.I. Antonov Penza State University of Architecture and Construction, ul. Germana Titova 28, 440028 Penza, Russia; e-mail: grey@pguas.ru;
V.A. Danilov Scientific and Technological Center of Unique Instrumentation, Russian Academy of Sciences, ul. Butlerova 15, 117342 Moscow, Russia;
B.A. Usievich Prokhorov General Physics Institute, Russian Academy of Sciences, ul. Vavilova 38, 119991 Moscow, Russia

Received 18 February 2020; revision received 18 March 2020
Kvantovaya Elektronika **50** (7) 623–628 (2020)
Translated by I.A. Ulitkin

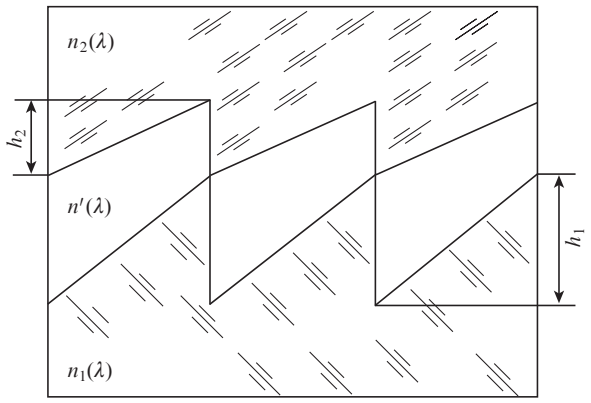

Figure 1. Three-layer double-relief sawtooth microstructure.

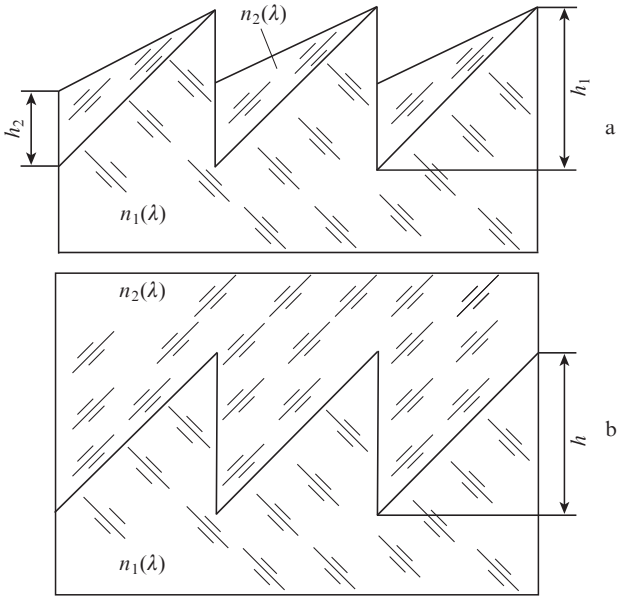

Figure 2. (a) Two-layer sawtooth microstructure with internal and external reliefs and (b) single-relief microstructure.

In the framework of the scalar diffraction theory (SDT), the dependence of DE of a multilayer sawtooth microstructure in the first working diffraction order on the wavelength λ and the angle of incidence of the light on the microstructure can be calculated by the formula [15]

$$\eta_s = \left\{\frac{\sin[\pi(1-\Delta l/\lambda)]}{\pi(1-\Delta l/\lambda)}\right\}^2, \quad (1)$$

where Δl is the optical path increment on a microstructure period.

In the case of a three-layer microstructure with two internal reliefs (Fig. 1), the optical path increment is described by the expression [11]

$$\Delta l = h_1\left[\sqrt{n_1^2(\lambda)-\sin^2\theta}-\sqrt{n'^2(\lambda)-\sin^2\theta}\right] - h_2\left[\sqrt{n_2^2(\lambda)-\sin^2\theta}-\sqrt{n'^2(\lambda)-\sin^2\theta}\right]. \quad (2)$$

Hereinafter, the light is assumed to be incident on the microstructure from the air from the side of a medium with a refractive index $n_1(\lambda)$, and the angle of incidence θ is measured from the normal to the substrate.

For two-layer microstructures with two internal reliefs (Fig. 1 at $n' = 1$), as well as with internal and external reliefs (Fig. 2a), the optical path increment can be calculated by the formula [11]

$$\Delta l = h_1\left[\sqrt{n_1^2(\lambda)-\sin^2\theta}-\cos\theta\right] - h_2\left[\sqrt{n_2^2(\lambda)-\sin^2\theta}-\cos\theta\right]. \quad (3)$$

Here, we immediately note that if, from the standpoint of SDT, the microstructures shown in Fig. 1 at $n' = 1$ and in Fig. 2a are absolutely similar, then in the rigorous diffraction theory they differ in the effective relief depth h_{eff}. The microstructures in Fig. 1 and Fig. 2a have $h_{\text{eff}} = h_1 + h_2$ and $h_{\text{eff}} = h_1$, respectively.

As for the optical path increment for a two-layer single-relief sawtooth microstructure (Fig. 2b), it is described by the expression [11]

$$\Delta l = h\left[\sqrt{n_2^2(\lambda)-\sin^2\theta}-\sqrt{n_1^2(\lambda)-\sin^2\theta}\right]. \quad (4)$$

It can be seen from expression (1) that one hundred percent DE ($\eta_s = 1$) is achieved under the condition $\Delta l(\lambda) = \lambda$. Even an approximate fulfilment of this condition in a wide spectral range is possible only at a certain ratio between the refractive indices and the dispersion coefficients of material layers. Expressions (3) and (4) imply a fundamental difference in the requirements for pairs of optical materials for single- and double-relief microstructures.

In the case of double-relief microstructures for the optical material whose refractive index is larger, the dispersion should also be greater, i.e., the difference in the refractive indices $n_2(\lambda) - n_1(\lambda)$ should decrease with decreasing wavelength (which can be achieved by a combination of a conventional flint- and crown-like materials). In the case of single-relief microstructures for the optical material whose refractive index is larger, the dispersion should be less, i.e., the difference $n_2(\lambda) - n_1(\lambda)$ should increase with increasing wavelength (which can be achieved by a combination of heavy crown- and light flint-like materials). Unfortunately, today, among technological and commercially available optical plastics, there are no pairs with the required ratio of optical constants. The situation has changed somewhat due to the heavy crowns available among the recently developed special brands of glass (glass for molded optics lenses, GMOL) [16]. Lenses made of these materials can be easily replicated by precision casting or stamping. Almost without a rise in prices, this technique can be employed to replicate lenses with a diffractive microrelief on a spherical or even aspherical surface (see, for example, [17]). However, even the best combinations of 'optical plastic–GMOL' make it impossible to sufficiently weaken the dependence of DE on the wavelength and the angle of incidence of the light at the DOE. Therefore, the search for new acceptable optical materials for both single-relief and double-relief microstructures is still underway. The purpose of this paper is to develop the necessary tools to facilitate the search for such materials, compare the characteristics of sawtooth microstructures composed of the already found combinations of optical materials, and evaluate the closeness these characteristics to the ideal ones.

2. Local and integral Q-factors of multilayer relief–phase diffraction microstructures

Within the framework of SDT, a preliminary estimate of the closeness of the characteristics of the multilayer sawtooth microstructure to the ideal ones is possible, in particular, by calculating the deviation of the optical path increment on one microstructure period $\delta\Delta l(\lambda_i)$ from the straight line $\Delta l_{\text{lin}}(\lambda_i)$, at each point of which $\eta_s = 1$:

$$\Delta l_{\text{lin}}(\lambda_i) = \lambda_i. \quad (5)$$

We will assume that the optical path increment on one microstructure period is expressed as

$$\Delta l(\lambda_i) = \Delta l_{\text{lin}}(\lambda_i) + \delta\Delta l(\lambda_i) = \lambda_i + \delta\lambda_i, \quad (6)$$

from which, taking into account condition (5), we obtain

$$\frac{\delta\Delta l(\lambda_i)}{\lambda_i} = \frac{\delta(\lambda_i)}{\lambda_i} = Q_i, \quad (7)$$

or, in accordance with expression (6),

$$Q_i = \frac{\Delta l(\lambda_i)}{\lambda_i} - 1. \quad (8)$$

The absolute value of Q_i determines how much η_s decreases for the wavelength λ_i. The negative consequence of the nonlinearity of the dependence $\Delta l(\lambda)$ within the entire working spectral range ($\lambda_{\min} \leqslant \lambda \leqslant \lambda_{\max}$) can be taken into account by using the rms value of Q_i, and this parameter is proposed to be called the integral Q-factor of the microstructure:

$$Q_{\text{int}} = \sqrt{\frac{1}{i_{\max}}\sum_1^{i_{\max}} Q_i^2}. \quad (9)$$

The expediency of using one or another evaluation parameter depends on the problem to be solved. If DOE is supposed to be introduced into a spectral device or into an imaging optical system and if diffraction of light into side orders is undesirable at any wavelength of the working spectral range, then the local Q-factor equal to the maximum absolute value of the parameter Q_i is the most adequate, i.e., $Q_{\text{loc}} = |Q_i|_{\max}$.

In the case of applying a DOE, for example, as a concentrator of solar energy, the most adequate parameter is the evaluation parameter Q_{int}.

The specific form of expressions (8) and (9) and the procedure for their use for the rational selection of combinations of optical materials, as well as for assessment of closeness of the characteristics of the microstructure composed of them to the ideal ones, depend on the type of microstructure. In the simplest case of a two-layer single-relief microstructure, expressions (8) and (9) at $\theta = 0$ have the form [18]

$$Q_i = \frac{\delta\Delta n(\lambda_i)}{\Delta n_{\text{lin}}(\lambda_i)}, \tag{10}$$

$$Q_{\text{int}} = \sqrt{\frac{1}{i_{\max}}\sum_{1}^{i_{\max}}\{[\Delta n(\lambda_i) - \Delta n_{\text{lin}}(\lambda_i)]/\Delta n_{\text{lin}}(\lambda_i)\}^2}, \tag{11}$$

where

$$\begin{aligned} &\delta\Delta n(\lambda_i) = \Delta n(\lambda_i) - \Delta n_{\text{lin}}(\lambda_i);\\ &\Delta n(\lambda_i) = n_2(\lambda_i) - n_1(\lambda_i);\\ &\Delta n_{\text{lin}}(\lambda_i) = \lambda_i \Delta n(\bar{\lambda})/\bar{\lambda}; \end{aligned} \tag{12}$$

and $\bar{\lambda}$ is the centre wavelength of the working spectral range. The relief depth in accordance with (4) is calculated by the formula

$$h = \bar{\lambda}/[n_2(\bar{\lambda}) - n_1(\bar{\lambda})]. \tag{13}$$

It is obvious that sorting out all optical materials from the corresponding catalogues of the world's leading manufacturers in order to minimise one of the selected evaluation parameters (Q_{loc} or Q_{int}) will make it possible to obtain the optimal combination of optical materials at a very low computational burden.

The procedure for determining the optimal combination of materials of a three-layer double-relief microstructure is somewhat more complicated. First of all, for the three initial optical materials and the initial relief depth $h_1 \geqslant 10\bar{\lambda}$ it is necessary to find the ratio of the depths of the reliefs, which ensures the optical path difference $\Delta l(\bar{\lambda}) = \bar{\lambda}$ and, therefore, $\eta_{\text{s}} = 1$ at a wavelength $\bar{\lambda}$ and normal incidence of the light ($\theta = 0$). From formula (2) we obtain

$$k = \frac{h_2}{h_1} = \frac{n_1(\bar{\lambda}) - n'(\bar{\lambda})}{n_2(\bar{\lambda}) - n'(\bar{\lambda})} - \frac{\bar{\lambda}}{h_1[n_2(\bar{\lambda}) - n'(\bar{\lambda})]}. \tag{14}$$

The evaluation parameter Q_i will be calculated by formula (8) using the expression

$$\Delta l(\lambda_i) = h_1\{[n_1(\lambda_i) - n'(\lambda_i)] - k[n_2(\lambda_i) - n'(\lambda_i)]\}. \tag{15}$$

For fixed parameters h_1 and k, it is necessary to obtain a set of Q_i values for some wavelengths satisfying the condition $\lambda_{\min} \leqslant \lambda_i \leqslant \lambda_{\max}$. This set will make it possible to determine the intermediate values of the local (Q_{loc}) and/or integral (Q_{int}) evaluation parameters. These values will characterise a maximum decrease in the DE of a microstructure made of the three selected optical materials within the specified spectral range at the initial relief depth h_1. An iterative process along h_1 will allow one to find the optimal relief depths that provide the smallest possible reduction in the DE of the microstructure made of the three selected optical materials. The search for all optical materials from the corresponding catalogues of the world's leading manufacturers will make it possible to obtain a microstructure for which the reduction in DE within a given spectral range is minimal. The transition to a two-layer ($n' = 1$) double-relief microstructure will only simplify the search for optical materials.

Further, it should be noted that Q-factors only allow for quick comparison of combinations of optical materials for a multilayer sawtooth microstructure and the selection of the most promising ones. A reliable estimate of the dependence of the DE on the angle of incidence of the light on the microstructure can be obtained only within the framework of the rigorous diffraction theory by solving Maxwell's equations with the corresponding boundary conditions, in particular the so-called rigorous coupled-wave analysis (RCWA) [19]. It should be noted that the modulus of the negative angle $|\psi_-|$ of incidence of the light on the microstructure and the positive angle ψ_+ of incidence, at which the DE, estimated by the RCWA method, decreases to the same value, can differ significantly. Therefore, for the evaluation angle, that is, for the maximum permissible angle Ψ, in this paper we use, as in [11–14], the smallest of the angles $|\psi_-|$ and ψ_+. As in the calculations in the framework of SDT, it is further assumed that the light is incident on the microstructure from air from the side of a medium with a refractive index $n_1(\lambda)$, and the angle Ψ is measured from the normal to the substrate.

Obviously, the estimate of the optimal depth of the microstructure relief and the maximum allowable angle of incidence of the light onto the microstructure depends on the choice of the corresponding criterion. If a DOE is supposed to be used in a spectral instrument or in an imaging optical system and if, as already noted, the diffraction of the light into side orders is undesirable at any wavelength of the working spectral range, then the criterion proposed in [12] is the most adequate. According to this criterion, the depths of the reliefs are considered optimal if they provide a maximum possible range of angles of incidence of the light in the selected spectral range, within which the DE (at the point of its minimum) does not fall below the minimum acceptable value equal to 0.95 of the maximum value of the DE at normal incidence of the light on the substrate microstructures ($\eta^{(\psi)}_{\text{EM min}}/\eta^{(\psi=0)}_{\text{EM max}} \geqslant 0.95$). This value guarantees the absence of not only a halo, but also of any other visually observable negative effect of lateral diffraction orders on the image quality formed by the optical system with a DOE. This criterion was successfully used in a number of works (see, for example, [13, 14, 20]).

If the selected combinations of optical materials and relief depths provide for a sawtooth microstructure that both Q-factors are equal to zero ($Q_{\text{loc}} = Q_{\text{int}} = 0$), then its DE $\eta^{(\psi=0)}_{\text{EM}}$, calculated by the RCWA method at normal incidence of the light, will differ from unity for all wavelengths of the working spectral range only by the magnitude of the Fresnel losses. The maximum permissible angle of incidence of the light (i.e., the evaluation angle Ψ corresponding to $\eta^{(\psi)}_{\text{EM min}}/\eta^{(\psi=0)}_{\text{EM max}} \geqslant 0.95$) at optimal relief depths will depend only on the type of microstructure and the ratio $P = \Lambda/h^{\text{opt}}_{\text{eff}}$ of its spatial period to the optimal effective relief depth. As a result, the family of DE dependences on the angle of incidence $\eta_{\text{EM}}(\psi)$ obtained at $Q_{\text{loc}} = Q_{\text{int}} = 0$ for a number of P values can be considered as the limiting characteristic of the microstructure of this type.

3. Comparative analysis of two-layer sawtooth microstructures

Two-layer single- and double-relief sawtooth microstructures composed of a number of pairs of optical materials, for which the maximum attenuation of the spectral and angular dependences of the DE are achieved, are presented in Table 1.

Within the spectral range and the range of angles of incidence of the light on the microstructure shown in Table 1, the normalised DE ($\eta_{\mathrm{EM\,min}}^{(\psi)}/\eta_{\mathrm{EM\,max}}^{(\psi=0)}$) estimated by the RCWA method does not fall below 0.95. The optimal relief depth and the maximum allowable angles of incidence of the light on the microstructure were obtained using two computer codes implementing the RCWA method: MC grating program and RCWA-PSUACE [22, 23]. In the last column of Table 1, each row indicates the work in which the microstructure composed of a given pair of optical materials was first studied. All two-layer double-relief microstructures have internal and external reliefs (see Fig. 2a).

The calculation results given in [11, 12, 20], as well as in this paper, were obtained using the dispersion formulae of the technologically and commercially available plastics, such as PMMA, POLYCARB (PC), POLYSTYR (PS), E48R and AL-6263 (OKP4HT), from the Misc and Zeon catalogues included in the Glasscat database of the Zemax optical design computer programme [24], as well as from the Optical plastic for molded lenses section of the Fiber Optic Center catalogue [25]. In addition, the dispersion formulae of the optical liquid Toluene and GMOL M-LAC8, presented in [26] and [27], respectively, were used in the calculations.

The single- and double-relief microstructures indicated in Table 1 demonstrate a certain correlation of Q-factors and the maximum allowable angles of incidence of light. Although the exact correspondence of the parameters obtained in the framework of the SDT and the angles calculated by the RCWA method is not observed.

The angular characteristics of single-relief microstructures composed of traditional optical materials (microstructures 1 and 2) are very close, but significantly inferior to those of microstructure 3. This microstructure, composed of nanocomposite materials and designed for an extended spectral range, has substantially larger allowable angles. In order to determine whether these angles are limiting for a two-layer single-relief sawtooth microstructure, it was proposed in [18] to replace one of the optical materials of the microstructure with a mathematical model that ensures the equality $Q_{\mathrm{loc}} = Q_{\mathrm{int}} = 0$. For the analysis we used microstructures 3 and 5, having minimum and maximum values of Q-factors and, therefore, the largest and smallest allowable angles of incidence of the light on the microstructure.

In model microstructure 4, as in microstructure 3, the lower layer onto which the light is incident from the air is made of a diamond in PMMA nanocomposite. Its dispersion coefficient is calculated by the formula

$$v_{\bar{\lambda}} = (n_{\bar{\lambda}} - 1)/(n_{\lambda_{\min}} - n_{\lambda_{\max}}), \tag{16}$$

Table 1. Parameters and angular characteristics of a number of single- and double-relief microstructures.

Microstructure type	Microstructure number	Optical materials of two layers with refractive indices n_1/n_2	Optimal depth h^{opt} or relief depth $h_1^{\mathrm{opt}}(h_2^{\mathrm{opt}})$/μm	$\lambda_{\min}-\lambda_{\max}$ /μm	Q_{loc}	Q_{int}	Ψ/deg	References
Single-relief	1	E48R/Toluene	15.09	0.4–0.7	0.1353	0.058	21.7 at $P = 10$ 28.3 at $P = 20$ 33.2 at $P = 30$	[11]
	2	AL-6263/M-LAC8	7.319	0.4–0.7	0.1366	0.061	13.0 at $P = 10$ 18.0 at $P = 20$ 21.8 at $P = 30$	[20]
	3	Nanocomposite: diamond in PMMA/ITO in PMMA	3.2	0.4–0.8	0.0452	0.016	36.3 at $P = 10$ 45.8 at $P = 20$ 50.0 at $P = 30$	[21]
	4	Nanocomposite: diamond in PMMA/mathematical model	3.2	0.4–0.8	0	0	37.7 at $P = 10$ 48.5 at $P = 20$ 53.5 at $P = 30$	[18]
	5	Nanocomposite: ZrO_2 in PMMA/PC	18.9	0.4–0.8	0.1792	0.070	4.0 at $P = 10$ 6.3 at $P = 20$ 15.7 at $P = 30$	[21]
	6	Nanocomposite: ZrO_2 in PMMA/mathematical model	24.6	0.4–0.8	0	0	25.6 at $P = 10$ 41.7 at $P = 20$ 47.3 at $P = 30$	[18]
Double-relief	7	PMMA/PC	15.1(11.7)	0.4–0.7	0.1283	0.058	3.2 at $P = 10$ 15.0 at $P = 20$ 16.8 при $P = 30$	[12]
	8	PMMA/mathematical model	15.1(11.79)	0.4–0.7	0	0	3.6 at $P = 10$ 26.5 at $P = 20$ 27.0 at $P = 30$	this paper
	9	E48R/PS	16.3(13.69)	0.4–0.7	0.1193	0.054	4.3 at $P = 10$ 15.5 at $P = 20$ 19.4 at $P = 30$	this paper
	10	E48R/mathematical model	16.3(13.76)	0.4–0.7	0	0	7.7 at $P = 10$ 26.1 at $P = 20$ 28.2 at $P = 30$	this paper

where $n_{\lambda_{\min}}$, $n_{\bar{\lambda}}$ and $n_{\lambda_{\max}}$ are the refractive indices of the medium at the minimum ($\lambda_{\min} = 0.4$ μm), centre ($\bar{\lambda} = 0.6$ μm) and maximum ($\lambda_{\max} = 0.8$ μm) wavelengths of the selected spectral range. Moreover, $n_{\bar{\lambda}} = 1.77097$ and $v_{\bar{\lambda}} = 23.533$. The upper model material ensures the equality $Q_{\text{loc}} = Q_{\text{int}} = 0$ and the same $\Delta n(\bar{\lambda})$ value as that of microstructure 3.

In model microstructure 6, as in microstructure 5, the lower layer onto which the light is incident from the air is made of a ZrO_2 in PMMA nanocomposite. Its refractive index at the centre wavelength is $n_{\bar{\lambda}} = 1.61748$, and the dispersion coefficient is $v_{\bar{\lambda}} = 18.824$. The upper model material ensures the fulfilment of the equality $Q_{\text{loc}} = Q_{\text{int}} = 0$ and the same value of $\Delta n(\bar{\lambda})$ as that of microstructure 5.

The refractive indices of the upper model materials of microstructures 4 and 6 were calculated by the formula

$$n_2(\lambda_i) = \frac{\lambda_i}{\bar{\lambda}}\Delta n(\bar{\lambda}) + n_1(\lambda_i). \tag{17}$$

Calculation and optimisation of the relief depths of microstructures 4 and 6 showed that the permissible angles of incidence of the light on microstructure 4 are greater than the corresponding angles of incidence on microstructure 6 (see Table 1). In this case, the normalised difference in the angles $\Delta\psi/\psi$ corresponding to the same value of P decreases with increasing this parameter. Indeed, if at $P = 10$ the value of $\Delta\psi/\psi \approx 47\%$, then at $P = 30$ it is only 13%. All this confirms the conclusion made in [18] that the allowable angles of incidence of the light on a single-relief microstructure are entirely determined by the relief depth h, that is, by the difference $\Delta n(\bar{\lambda}) = n_2(\bar{\lambda}) - n_1(\bar{\lambda})$[see formula (13)]. The materials of microstructure 4 provide the maximum possible difference $\Delta n(\bar{\lambda})$ for the known optical materials (suitable for the manufacture of DOEs) and, therefore, the minimum depth h^{opt}. This allows one to consider the obtained maximum allowable angles of incidence on microstructure 4 as limiting for two-layer single-relief sawtooth microstructures. Here, we immediately recall that the assessment of the optimal depth of the microstructure relief and the maximum allowable angles of incidence of the light on this microstructure depends on the choice of the corresponding criterion. All the above estimates are obtained for the criterion $\eta^{(\psi)}_{\text{EM min}}/\eta^{(\psi=0)}_{\text{EM max}} \geqslant 0.95$. Finally, returning to microstructure 3, there is every reason to state that its angular characteristics are very close to the maximum possible.

As for the nanocomposite materials that were used to assemble microstructures 3 and 5, the dependences of their refractive indices on the wavelength are described by the formula

$$n^2 - 1 = \frac{K_1\lambda^2}{\lambda^2 - L_1} + \frac{K_2\lambda^2}{\lambda^2 - L_2} + \frac{K_3\lambda^2}{\lambda^2 - L_3}. \tag{18}$$

The values of the coefficients K_{1-3} and L_{1-3}, kindly provided by the authors of work [21], are summarised in Table 2.

A detailed description of the approaches to the design of optical nanocomposites is presented by Werdehausen et al. [28], who showed, in particular, that the right choice of nanoparticle sizes makes it possible to exclude the effect of incoherent scattering which is unacceptable for optical elements.

It should be noted here that Table 1 does not contain two-layer single-relief microstructures, which were made of nanocomposite materials with nanoparticles of zirconium dioxide and titanium [29]. Also, Table 1 did not include the microstructure composed of two new types of UV-curable resins [30]. This is due to the fact that the dispersion formulas of the listed materials are not published yet and are still unavailable. As a result, it is impossible, using single evaluation parameters, to compare the results of these developments with the results presented in Table 1, and to assess the closeness of the spectral and angular characteristics of microstructures to the ideal ones for microstructures of these types.

Table 2. Coefficients of the dispersion formula (18) of nanocomposite optical materials.

Material	K_1	K_2	K_3	L_1	L_2	L_3
Diamond in PMMA	1.68193	0.39121	−1.45947	0.00805	0.02188	−906.42838
ITO in PMMA	1.21406	0.48463	2.98136	0.00489	0.04373	5.19483
ZrO_2 in PMMA	1.17846	0.37802	0.00570	0.01431	0.00967	−3.36306

The angular characteristics of double-relief microstructures made of traditional optical materials (7 and 9) are quite comparable, but are significantly inferior to those of microstructure 3. In order to assess how the angular characteristics of microstructures 7 and 9 differ from the maximum possible characteristics of two-layer double-relief microstructures, we use model microstructures 8 and 10 as was done in the analysis of single-relief microstructures. When composing them, the optical materials of the lower layers remained the same as those of microstructures 7 and 9, and the materials of the upper layers were replaced by the corresponding mathematical model, which ensures the fulfilment of the condition $Q_{\text{loc}} = Q_{\text{int}} = 0$. The refractive indices of model materials were calculated by the formula

$$n_2(\lambda_i) = \frac{h_1}{h_2}[n_1(\lambda_i) - 1] - \frac{\lambda_i}{h_2} + 1. \tag{19}$$

In this case, the relief depths h_1 of the lower layers of microstructures 8 and 10 were taken equal to the depths h_1 of the microstructures 7 and 9, respectively, and the depths h_2 of the upper layers were optimised.

As a result, we found that the maximum allowable angles of incidence of the light on model microstructures are quite close, and the allowable angles of incidence of the light inside the lower layer of these microstructures, especially for large spatial periods, are almost the same. Indeed, the maximum permissible angle of incidence of the light inside the lower layer of microstructure 8 at $P = 30$ is 17.5°, while the corresponding angle of microstructure 10 is 17.75°. Therefore, the maximum allowable angles of incidence of the light on model microstructures 8 and 10 presented in Table 1 can be considered as limiting angles for two-layer double-relief sawtooth microstructures. These angles are approximately one and a half times the maximum allowable for microstructures 7 and 9. This is significantly different from the calculation results for single-relief microstructures composed of traditional optical materials that allow precision casting or stamping.

4. Conclusions

The procedures for calculating the local and integral Q-factors that are used in this work for multilayer double-relief sawtooth-shaped diffraction microstructures provide the oppor-

tunity to choose the best combinations of optical materials for any type of microstructures at a very low computation burden.

The approach proposed by the authors to the study of multilayer relief–phase diffraction microstructures, based on the combined use of Q-factors and the RCWA method, made it possible to establish the following:

1. In the visible spectral range (0.4–0.7 μm), the maximum allowable angles of incidence of the light on the microstructure, achieved for two-layer single-relief microstructures made of traditional materials and allowing precision casting or stamping of optical materials, exceed by no more than 15%–20% the corresponding angles for two-layer double-relief microstructures composed of technologically advanced and commercially available optical plastics. At the same time, the limiting angles of incidence of the light on two-layer single-relief microstructures are almost two times higher than the corresponding angles for two-layer double-relief microstructures.

2. Technological and commercially available plastics make it possible to compose two-layer double-relief microstructures with spectral and angular characteristics close to the maximum possible values for these types of microstructures.

3. Of practically significant material combinations for two-layer single-relief microstructures, the 'optical plastic–GMOL' pairs are the best; however, the maximum allowable angles of incidence of the light on the microstructures composed of them are significantly smaller than the limiting angles for these types of microstructures.

4. Spectral and angular characteristics that are as close as possible to the limiting ones for two-layer single-relief microstructures can be obtained by their arrangement from nanocomposite optical materials.

Acknowledgements. The authors are grateful to the authors of Ref. [21] for the opportunity to use the dispersion formulae of the nanocomposite materials they created.

This work was supported by the Russian Science Foundation (Project No. 20-19-00081).

References

1. Flores A., Wang M.R., Yang J.J. *Appl. Opt*. **43**, 5618 (2004).
2. Greisukh G.I., Ezhov E.G., Levin I.A., Stepanov S.A. *Appl. Opt*., **49**, 4379 (2010).
3. Jia H., Wang D. *J. Soc. Inf. Disp*., **19**, 265 (2011).
4. Greisukh G.I., Ezhov E.G., Levin I.A., Stepanov S.A. *Computer Optics*, **35**, 473 (2011) [*Komp'yuternay Opt*., **35**, 473 (2011)].
5. Greisukh G.I., Ezhov E.G., Kalashnikov A.V., Stepanov S.A. *Appl. Opt*., **51**, 4597 (2012).
6. Lukin A., Mustafin K., Rafikov R. RF Patent No. 1271240 (1985).
7. Lukin A.V. *Opt. Zh*., **74**, 80 (2007).
8. Ebstein S.T. *Proc. SPIE*, **2404**, 211 (1995).
9. http://www.jeos.org/index.php/jeos_rp/article/view/176.
10. Greisukh G.I., Danilov V.A., Ezhov E.G., Levin I.A., Stepanov S.A., Usievich B.A. *Opt. Commun*., **338**, 54 (2015).
11. Greisukh G.I., Danilov V.A., Ezhov E.G., Stepanov S.A., Usievich B.A. *Opt. Spectrosc.*, **118**, 964 (2015) [*Opt. Spektrosk*., **118**, 997 (2015)].
12. Greisukh G.I., Yezhov U.G., Stepanov S.A. *J. Opt. Technol*., **82** (5), 308 (2015) [*Opt. Zh*., **82**, 56 (2015)].
13. Greisukh G.I., Danilov V.A., Stepanov S.A., Antonov A.I., Usievich B.A. *Opt. Spectrosc*., **124**, 98 (2018) [*Opt. Spektrosk*., **124**, 100 (2018)].
14. Greisukh G.I., Danilov V.A., Stepanov S.A., Antonov A.I., Usievich B.A. *Opt. Spectrosc*., **125**, 60 (2018) [*Opt. Spektrosk*., **125**, 57 (2018)].
15. Buralli D.A., Morris G.M., Rogers J.R. *Appl. Opt*., **28**, 976 (1989).
16. http://www.hoya-opticalworld.com/english/products/moldlenses.html.
17. http://www.edmundoptics.com.
18. https://iopscience.iop.org/article/10.1088/2040-8986/ab90ce/pdf.
19. Moharam M.G., Gaylord T.K. *J. Opt. Soc. Am*. **72**, 1385 (1982).
20. Greisukh G.I., Danilov V.A., Antonov A.I., Stepanov S.A., Usievich B.A. *Computer Optics*, **42**, 38 (2018) [*Komp'yuternay Opt*., **42**, 38 (2018)].
21. Werdehausen D., Burger S., Staude I., Pertsch Th., Decker M. *Optica*, **6**, 1031 (2019).
22. Lyndin N.M. *Modal and C Methods Grating Design and Analysis Software*; http://www.mcgrating.com.
23. Greisukh G.I., Antonov A.I., Yezhov E.G. *Opt. Zh*., **86**, 3 (2019).
24. https://www.radiantvisionsystems.com/.
25. http://focenter.com/wp-content/uploads/2015/05/AngstromLink-AL-6261-6263-6264-6265.pdf.
26. Marvin J., Weber M.J. *Handbook of Optical Materials* (Boca Raton: CRC Press, 2003).
27. http://www.hoya-opticalworld.com/english/datadownload/index.html.
28. Werdehausen D., Staude I., Burger S., Petschulat J., Scharf T., Pertsch Th., Decker M. *Opt. Mater. Express*, **8**, 3456 (2018).
29. Korenaga T., Ando T., Okada Y., et al. *Opt. Rev*. **21**, 737 (2014).
30. Nakamura T., Suzuki K., Inokuchi Y., Nishimura S. *Opt. Eng*., **58**, 085103 (2019).